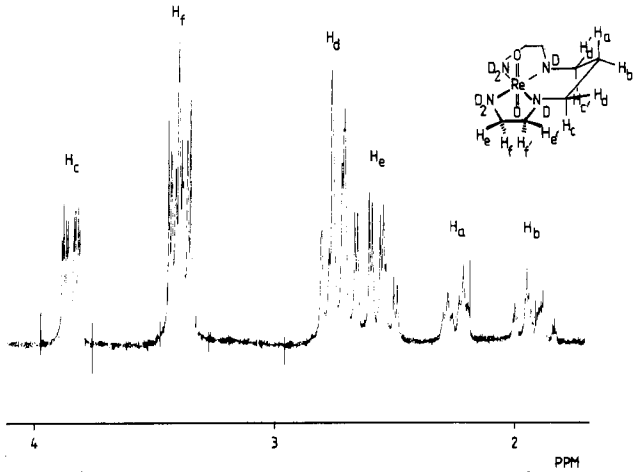

Figure 2. ^1H NMR spectrum (298 K, D_2O, 250 MHz) of $[L^2ReO_2]PF_6$. Proton assignments were made with the aid of selective decoupling experiments and a 2D COSY spectrum.

For the complexes $[L^2ReO_2]Cl$ and $[L^3ReO_2]X$ (X = Cl, OAc), a mixture of the trans-racemic and trans-meso diastereoisomers was obtained as deduced most clearly from the ^{13}C NMR data.[12] With $[L^2ReO_2]Cl$, for example, eight resonances were observed: four each of the C_2-symmetric racemic and the σ-symmetric meso diastereoisomers. When the hexafluorophosphate salt was crystallized, only one diastereoisomer was isolated. It was stable in aqueous solution for up to 1 week (in the presence and absence of free ligand), in the pH regime 5–8, and its proton NMR spectrum is shown in Figure 2, which highlights that the methylene protons are all diastereotopic. At this stage it is not possible to assign the configuration of the pure diastereoisomer isolated: a crystallographic analysis or an attempted resolution is required. For the corresponding complexes with L^3, both diastereoisomers were observed by ^{13}C NMR spectroscopy. Each diastereoisomer should give rise to five distinct resonances, but only eight were observed due to the anisochrony of two pairs of peaks. Fractional crystallization, with different anions, from water failed to separate the diastereoisomers.

Conclusion

Reaction of $ReOCl_3(PPh_3)_2$ with the acyclic tetraamine ligands L^1–L^3 affords a quick and convenient synthesis of the *trans*-$[L^nReO_2]$ cationic complexes. With L^2 and L^3, the resultant dioxorhenium(V) complexes are stable in aqueous solution over a wide range of pH, reversibly protonate in 6 M HCl, and do not undergo ligand-exchange reactions. The ^1H and ^{13}C NMR spectra reveal that a single diastereoisomer of $[L^2ReO_2]^+$ may be easily separated as its hexafluorophosphate salt, while the diastereoisomers of the acetate and chloro salts of $[L^3ReO_2]^+$ were not separable by fractional crystallization.

Acknowledgment. We thank Celltech plc and SERC for support and Dr. M. Jones for his assistance with the FAB mass spectra.

Registry No. $[L^1ReO_2]Cl$, 116784-22-6; $[L^2ReO_2]PF_6$, 116839-34-0; *trans-rac*-$[L^2ReO_2]Cl$, 116784-23-7; *trans-meso*-$[L^2ReO_2]Cl$, 116839-36-2; *trans-rac*-$[Cl^3ReO_2]Cl$, 116784-24-8; *trans-meso*-$[L^3ReO_2]Cl$, 116839-35-1; *trans-rac*-$[L^3ReO_2]PF$, 116784-30-6; *trans-meso*-$[L^3ReO_2]PF_6$, 116839-38-4; $[L^2ReO(OH)^{2+}$, 116784-25-9; $[L^3RO(OH)]^{2+}$, 116784-26-0; $[L^2ReO(OH_2)]^{3+}$, 116784-27-1; $[L^3RO(OH_2)]^{3+}$, 116784-28-2; $[Re(en)_2O_2]^+$, 14405-69-7; *trans*-$ReOCl_3(PPh_3)_2$, 34248-12-9.

Contribution from the Department of Physical Chemistry, The Hebrew University of Jerusalem, Jerusalem 91904, Israel, and Nuclear Research Centre Negev, R. Bloch Coal Research Center, and Chemistry Department, Ben-Gurion University of the Negev, Beer Sheva, Israel

Formation and Decomposition of Transient Complexes with a Copper–Carbon σ-Bond in the Reaction of Copper(I) Phenanthroline with Aliphatic Free Radicals. A Pulse Radiolysis Study

Sara Goldstein,*,† Gidon Czapski,† Haim Cohen,*,‡ and Dan Meyerstein§

Received May 17, 1988

The oxidation of copper(I) phenanthroline by $^{\bullet}CH_2CH_2OH$ and $^{\bullet}CH_2C(CH_3)_2OH$ free radicals yields ethylene and 2-methylpropene, respectively. During this process transients with a copper–carbon σ-bond have been observed with an absorbance similar to that of copper(I) phenanthroline in the visible region. Rate constants for the formation of these transients are estimated to be larger than 10^{10} M^{-1} s^{-1}. These intermediates decompose via a β-hydroxyl elimination reaction with specific rate constants of $(1.7 \pm 0.4) \times 10^3$ and $(1.1 \pm 0.3) \times 10^4$ s^{-1} for $^{\bullet}CH_2C(CH_3)_2OH$ and $^{\bullet}CH_2CH_2OH$ in the pH range 4–10, respectively. The mechanism of the decomposition is discussed, and a stability constant for the ligation of $^{\bullet}CH_2C(CH_3)_2OH$ and $^{\bullet}CH_2CH_2OH$ to the cuprous complex is estimated to be larger than 6×10^6 M^{-1}.

Introduction

Reactions between copper ions and aliphatic free radicals occur in metal-catalyzed oxidations of organic compounds as well as in many biochemical processes.[1-4] Mechanistic studies indicate that aliphatic free radicals ($R^{\bullet}$) react with cupric and cuprous ions via a mechanism that involves the formation of short-lived intermediates having a copper–carbon σ-bond:

$$Cu_{aq}^{2+} + R^{\bullet} \rightarrow Cu^{III}\text{–}R \quad (1)$$

$$Cu_{aq}^{+} + R^{\bullet} \rightarrow Cu^{II}\text{–}R \quad (2)$$

With use of the pulse radiolysis technique, the chemical properties of several short-lived intermediates formed in reactions 1 and 2 have been studied. It was found that Cu_{aq}^{+} reacts faster than Cu_{aq}^{2+} with aliphatic free radicals to yield transients with a copper–carbon σ-bond with specific rate constants approaching

* To whom correspondence should be addressed.
† The Hebrew University of Jerusalem.
‡ Nuclear Research Centre Negev and R. Bloch Coal Research Center, Ben-Gurion University of the Negev.
§ Chemistry Department and R. Bloch Coal Research Center, Ben-Gurion University of the Negev.

(1) Kochi, J. K. In *Free Radicals*; Kochi, J. K., Ed.; Wiley: New York, 1973; Vol. 1, Chapter II.
(2) Kochi, J. K. *Acc. Chem. Res.* **1974**, *7*, 351.
(3) Walling, C.; Kats, S. *J. Am. Chem. Soc.* **1971**, *93*, 4275.
(4) Walling, C. *Acc. Chem. Res.* **1975**, *8*, 2125.

0020-1669/88/1327-4130$01.50/0

the diffusion control limit.[5-12] For example, $k_1 = (5 \pm 2) \times 10^6$ and $(3 \pm 1) \times 10^7$ M^{-1} s^{-1} for the formation of the transients with the copper–carbon σ-bond in the reaction of Cu_{aq}^{2+} with $^{\bullet}CH_2C(CH_3)_2OH$ and $^{\bullet}CH_2CH_2OH$, respectively.[6,8] From experiments in which Cu_{aq}^{+} was formed in situ by the pulse, k_2 was determined indirectly to be $(2.6 \pm 0.9) \times 10^{10}$ and $(1.9 \pm 0.6) \times 10^{10}$ M^{-1} s^{-1} for $^{\bullet}CH_2C(CH_3)_2OH$ and $^{\bullet}CH_2CH_2OH$, respectively.[7] More recently, it has been shown that one can extend the range of reactions that can be studied by preparing solutions of Cu_{aq}^{+} through the reduction of Cu_{aq}^{2+} by Cr_{aq}^{2+}, and hence reaction 2 and the spectrum of Cu^{II}–R can be followed directly.[11,12] By use of this technique, k_2 was determined to be $(4.5 \pm 1.1) \times 10^9$ M^{-1} s^{-1} in the case of $^{\bullet}CH_2C(CH_3)_2OH$.[13] With the use of this technique, the β-hydroxyl elimination reaction was also studied.

$$Cu^{II}—CH_2C(CH_3)_2OH^{+} \rightarrow Cu_{aq}^{2+} + CH_2{=}C(CH_3)_2 + OH^{-} \quad (3)$$

It was found that the yield of 2-methylpropene was equal to the yield of $^{\bullet}CH_2C(CH_3)_2OH$. Reaction 3 was found to be pH-dependent with k_3 $(s^{-1}) = 5 \times 10^4 + 8.6 \times 10^7[H^+]$.[13] It has also been reported that $^{\bullet}CH_2CH_2OH$ radical oxidizes Cu_{aq}^{+} with k_4 $(s^{-1}) = 3.2 \times 10^3 + 3.8 \times 10^7[H^+]$.[7]

$$Cu^{II}—CH_2CH_2OH^{+} \rightarrow Cu_{aq}^{2+} + CH_2{=}CH_2 + OH^{-} \quad (4)$$

We decided to investigate to what extent ligands that strongly bind copper ions influence the kinetics of the formation and the decomposition of the transient complexes with a copper–carbon σ-bond in the case of $^{\bullet}CH_2C(CH_3)_2OH$ and $^{\bullet}CH_2CH_2OH$ radicals. 1,10-Phenanthroline (OP) has been chosen as a ligand for copper for several reasons: (a) OP binds Cu^{II} and Cu^{I} very strongly.[14] (b) Copper(I) phenanthroline ($(OP)_2Cu^{+}$) is a tetrahedral complex, and therefore no Cu^{I} π-complex can be formed; e.g., the π-complex of Cu^{I} with the double bond of 2-methylpropene or ethylene. (c) $(OP)_2Cu^{+}$ absorbs very strongly in the visible region due to a metal to ligand charge-transfer band (ϵ_{430} = 7800 M^{-1} cm^{-1}),[14,15] and thus it is easy to follow its concentration. (d) $(OP)_2Cu^{II}$–$CH_2C(CH_3)_2OH^{+}$ and $(OP)_2Cu^{II}$–$CH_2CH_2OH^{+}$ may serve as models for reactions of $(OP)_2Cu^{+}$ with free radicals formed in biological processes, e.g., radicals derived from glycerol, glucose, ATP, DNA, etc. Intermediates with a copper–carbon σ-bond thus formed may undergo β-hydroxyl elimination reactions causing degradation of the biological molecules. Indeed, it has already been demonstrated that $(OP)_2Cu^{+}$ with H_2O_2 has an artificial DNase activity that rapidly cleaves double-stranded DNA.[16-18] This reagent cleaves DNA in a manner different from that of OH• radicals formed homogenously by γ-radiation.[19] One of the explanations for this study is that Cu^{III} or OH• radicals are formed via the modified Fenton reaction at the vicinity of the target site. A DNA radical formed by these strong oxidizing species may react with Cu^{I}, yielding an intermediate with a copper–carbon σ-bond that may undergo a β-hydroxyl elimination reaction. The formation of a double bond is a process that in most biological systems is irreversible, and therefore, such a reaction may cause an irreversible DNA damage.

Experimental Section

Materials. All chemicals were of analytical grade and were used as received: $CuSO_4 \cdot 7H_2O$, NaOH, $HClO_4$, hydrazine sulfate (Merck), 1,10-phenanthroline, *tert*-butyl alcohol (Fluka), and N_2O; helium and ethylene (Matheson). All solutions were prepared with distilled water that was further purified by using a Millipore setup. Solutions of $(OP)_2Cu^{2+}$ were prepared by mixing cupric sulfate with 2–2.2 equiv of the ligand. Under these conditions the major species formed is $(OP)_2Cu^{2+}$.[14] With higher ratios of ligand to metal, the concentration of $(OP)_3Cu^{2+}$ cannot be neglected,[14] and it reacts differently from $(OP)_2Cu^{2+}$.[20] Solutions of $(OP)_2Cu^{+}$ were prepared through the reduction of $(OP)_2Cu^{2+}$ by hydrazine (a four-electron reductant) in deaerated solutions at pH 7. A stock solution of 0.01 M hydrazine was prepared, and an appropriate amount was added to N_2O-saturated solutions containing $(OP)_2Cu^{2+}$ and *tert*-butyl alcohol at pH 7. The reduction reaction was completed within 3–4 h, and the concentration of $(OP)_2Cu^{+}$ was determined spectrophotometrically by using ϵ_{430} = 7800 M^{-1} cm^{-1}. The pH was adjusted with $HClO_4$ and NaOH.

Irradiations. Pulse radiolysis experiments were carried out with a Varian 7715 linear accelerator at The Hebrew University of Jerusalem. The pulse duration was 0.05–1.5 μs with a 200-mA current of 5-MeV electrons. Irradiations were done in a 2- or 4-cm Spectrosil cell by using three light passes. A 150-W Xenon arc produced the analyzing light. The detection system included a Bausch & Lomb grating monochromator Model D330/D331 Mk.II and an IP28 photomultiplier. The signal was transferred through a SONY/TEXTRONIX 390AD programmable digitizer to a micro PDP-11/24 computer, which operated the whole pulse radiolysis system. An N_2O-saturated solution containing 1 mM KSCN was used for dosimetry. The yield of $(SCN)_2^{-}$ was measured by taking ϵ_{475} = 7600 M^{-1} cm^{-1} and assuming $G((SCN)_2^{-}) = 6$. The dose per pulse was set so that the initial free radical concentration was 1–11 μM. The values of the molar extinction coefficients calculated from dosimetry measurements have an error limit of at least 10% due to scatter in the repetition of the pulse intensity and due to uncertainties in G values. Large doses of irradiation for product analysis have been delivered into small cylindrical glass bulbs (12-mL volume) filled with 10 mL of deaerated solutions and sealed with a rubber septum. In this case the Fricke dosimeter was used for determining the total concentration of the free radicals by taking $G(Fe^{3+}) = 15.6$ and ϵ_{302} = 2197 M^{-1} cm^{-1}.

A ^{137}Cs source (Radiation Machinary Co. Model M3813) with a dose rate of 1.25 krads/min was used for low dose rate experiments and product analysis. The solutions were irradiated in glass bottles closed with rubber septa. Dosimetry was done with the Fricke dosimeter.

Analysis. The yield of 2-methylpropene and ethylene was determined by gas chromatography. The gas samples were taken through the rubber septa with gastight syringes and were separated on a Peropapak Q column with 30 mL/min of helium carrier gas at 180 °C by using a Varian 3700 TCD chromatograph.

Production of Free Radicals. The radiolysis of water may be described by

$$H_2O \rightsquigarrow e_{aq}^{-}\ (2.65),\ OH^{\bullet}\ (2.65),\ H^{\bullet}\ (0.6),\ H_2\ (0.45),\ H_2O_2\ (0.75) \quad (5)$$

The numbers in parentheses are G values, which represent the number of molecules formed/100 eV of energy absorbed in the solution.[21] The precise values of G are slightly dependent on solute concentrations. At high concentrations the yield of the free radicals increases and that of H_2 and H_2O_2 decreases.[21] The free radicals formed are homogeneously distributed in solution within less than 100 ns after the radiation is absorbed.

In N_2O-saturated solutions ($[N_2O]$ = 0.022 M), e_{aq}^{-} reacts with N_2O according to reaction 6. After the completion of reaction 6, 90% of all

$$e_{aq}^{-} + N_2O \xrightarrow{H_2O} N_2 + OH^{-} + OH^{\bullet} \quad (6)$$
$$k_6 = 9.1 \times 10^9\ M^{-1}\ s^{-1}\ [22]$$

the primary radicals are present as OH• radicals, the rest being H• atoms.

(5) Freiberg, M.; Meyerstein, D. *J. Chem. Soc., Chem. Commun.* **1973**, 934.
(6) Freiberg, M.; Meyerstein, D. *J. Chem. Soc., Faraday Trans. 1* **1980**, *76*, 1825.
(7) Freiberg, M.; Mulac, W. H.; Schmidt, K. H.; Meyerstein, D. *J. Chem. Soc., Faraday Trans. 1* **1980**, *76*, 1838.
(8) Buxton, G. V.; Green, J. E. *J. Chem. Soc., Faraday Trans. 1* **1978**, *74*, 697.
(9) Buxton, G. V.; Green, J. E.; Sellers, R. M. J. *J. Chem. Soc., Dalton Trans.* **1976**, 2160.
(10) Das, S.; Johnson, G. R. A. *J. Chem. Soc., Faraday Trans. 1* **1980**, *74*, 1779.
(11) Cohen, H.; Meyerstein, D. *Inorg. Chem.* **1986**, *25*, 1506.
(12) Cohen, H.; Meyerstein, D. *Inorg. Chem.* **1987**, *26*, 2342.
(13) Cohen, H.; Meyerstein, D., submitted for publication.
(14) James, B. R.; Williams, R. J. P. *J. Chem. Soc.* **1961**, 2007.
(15) Goldstein, S.; Czapski, G. *J. Am. Chem. Soc.* **1983**, *105*, 7276.
(16) Que, B. G.; Downey, K. M.; So, A. G. *Biochemistry* **1980**, *19*, 5987.
(17) Marshall, L. E.; Graham, D. R.; Reich, K. A.; Sigman, D. S. *Biochemistry* **1981**, *20*, 244.
(18) Thomas, E. G.; Sigman, D. S. *J. Am. Chem. Soc.* **1987**, *109*, 2846.
(19) Aronovitch, J.; Godinger, D.; Samuni, A.; Czapski, G. *Free Radical Res. Commun.* **1987**, *2*, 241.
(20) Goldstein, S.; Czapski, G. *J. Am. Chem. Soc.* **1986**, *108*, 2244.
(21) Matheson, M. S.; Dorfman, L. M. *Pulse Radiolysis*; MIT Press: Cambridge, MA, 1969.
(22) Janata, E.; Schuler, R. H. *J. Phys. Chem.* **1982**, *68*, 2078.

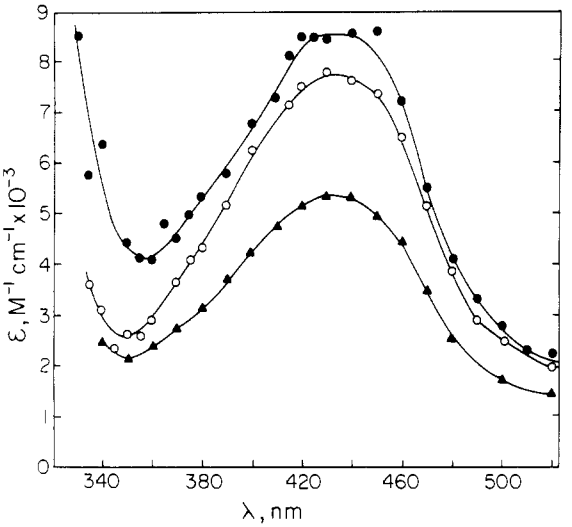

Figure 1. Absorption spectra of $(OP)_2Cu^+$ and transients having a copper–carbon bond. ○: $(OP)_2Cu^+$; solutions contained 1×10^{-4} M $(OP)_2Cu^{2+}$ and 0.1 M formate at pH 7 and were oxygen-saturated. ●: $(OP)_2Cu^{II}$–$CH_2C(CH_3)_2OH^+$; solutions contained 2×10^{-4} M $(OP)_2Cu^{2+}$ and 0.1 M *tert*-butyl alcohol at pH 7 and were He-saturated. △: $(OP)_2Cu^{II}$–$CH_2CH_2OH^+$; solutions contained 1×10^{-4} M $(OP)_2Cu^{2+}$ at pH 7 and were ethylene-saturated.

When $(CH_3)_3COH$ is added to the solution, all the primary radicals are converted into $^{\bullet}CH_2C(CH_3)_2OH$ via reactions 6 and 7. In the absence

$$OH^{\bullet}/H^{\bullet} + (CH_3)_3COH \rightarrow H_2O/H_2 + {}^{\bullet}CH_2(CH_3)_2OH \quad (7)$$
$$k_{OH} = 4.2 \times 10^8\ M^{-1}\ s^{-1},^{23} \quad k_H = 8 \times 10^4\ M^{-1}\ s^{-1}\ ^{24}$$

of any scavenger for the radical, it dimerizes in a second-order reaction:

$$2{}^{\bullet}CH_2C(CH_3)_2OH \rightarrow (CH_2C(CH_3)_2OH)_2 \quad (8)$$
$$2k_8 = 1.4 \times 10^9\ M^{-1}\ s^{-1}\ ^{25}$$

In He-saturated solutions containing *tert*-butyl alcohol and copper(II) complexes, e_{aq}^- reduces the complexes with rates approaching the diffusion-control limit ($k = (1–3) \times 10^{10}\ M^{-1}\ s^{-1}$),[26] and $H^{\bullet}$ and $OH^{\bullet}$ produce the $^{\bullet}CH_2C(CH_3)_2OH$ radical.

In ethylene-saturated solutions ($[CH_2{=}CH_2] = 0.013$ M) containing copper(II) complexes, e_{aq}^- reduces the complexes, and $OH^{\bullet}$ and $H^{\bullet}$ are converted into $^{\bullet}CH_2CH_2OH$ and $^{\bullet}CH_2CH_3$ radicals via reactions 9 and 10.

$$OH^{\bullet} + CH_2{=}CH_2 \rightarrow {}^{\bullet}CH_2CH_2OH \quad (9)$$
$$k_9 = 1.8 \times 10^9\ M^{-1}\ s^{-1}\ ^{23}$$

$$H^{\bullet} + CH_2{=}CH_2 \rightarrow {}^{\bullet}CH_2CH_3 \quad k_{10} = 3.2 \times 10^9\ M^{-1}\ s^{-1}\ ^{24} \quad (10)$$

Results

A. The *tert*-Butyl Alcohol System. When He-saturated solutions containing 0.1–0.5 mM $(OP)_2Cu^{2+}$ and 0.01–1 M *tert*-btyl alcohol at pH 7 are irradiated, the formation of an unstable intermediate is observed with a spectrum similar to that of $(OP)_2Cu^+$ (Figure 1). The rate of the formation of this intermediate was too fast to be measured under these conditions, and its yield was independent of $[(OP)_2Cu^{2+}]$ (Table I). We attribute this intermediate to the formation of the unstable complex of $(OP)_2Cu^{II}$–$CH_2C(CH_3)_2OH^+$ via reactions 11 and 12. The rate

$$e_{aq}^- + (OP)_2Cu^{2+} \rightarrow (OP)_2Cu^+ \quad (11)$$

$$^{\bullet}CH_2C(CH_3)_2OH + (OP)_2Cu^+ \rightarrow (OP)_2Cu^{II}\text{–}CH_2C(CH_3)_2OH^+ \quad (12)$$

of the decomposition of the intermediate obeys a first-order rate law, slightly depends on the pulse intensity, and is independent

(23) Farhataziz; Ross, A. B. *Natl. Stand. Ref. Data Ser.* (*U.S., Natl. Bur. Stand.*) **1977**, *NSRDS-NBS*, 59.
(24) Anbar, M.; Farhataziz; Ross, A. B. *Natl. Stand. Ref. Data Ser.* (*U.S., Natl. Bur. Stand.*) **1975**, *NSRDS-NBS*, 51.
(25) Ross, A. B.; Neta, P. *Natl. Stand. Ref. Data Ser.* (*U.S., Natl. Bur. Stand.*) **1982**, *NSRDS-NBS*, 70.
(26) Anbar, M.; Banbeneck, M.; Ross, A. B. *Natl. Stand. Ref. Data Ser.* (*U.S., Natl. Bur. Stand.*) **1973**, *NSRDS-NBS*, 43.

Table I. Values for the Observed Rate Constant of the Decomposition (k_d) of $(OP)_2Cu^{II}$–$CH_2C(CH_3)_2OH^+$ in He-Saturated Solutions Containing 0.1 M *tert*-Butyl Alcohol as a Function of Various Conditions[a]

$[Cu^{2+}]$, 10^{-4} M	dose, 10^{-6} M	λ, nm	pH	OD_0	OD_∞	k_d, $10^3\ s^{-1}$
1	1.3	430	7	0.067	0.017	1.5
1	1.3	500	7	0.020	0.010	1.7
1	3.3	430	7	0.196	0.110	2.6
2	1.3	430	7	0.061	0.019	1.4
2	1.3	370	7	0.033	0.010	1.3
2	1.3	430	4	0.062	0.021	1.2
2	1.3	430	10	0.071	0.022	1.9
5	1.3	430	7	0.065	0.035	2.0
5	3.3	430	7	0.200	0.136	2.8

[a] The optical path length was 12.1 cm.

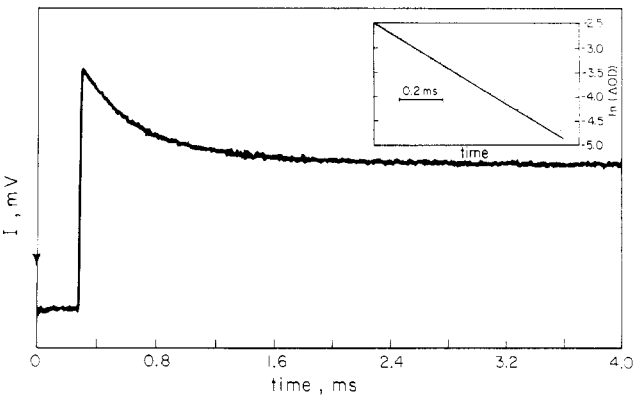

Figure 2. Typical kinetic plot of a pulse-radiolyzed He-saturated solution containing 0.1 mM $(OP)_2Cu^{2+}$ and 0.1 M *tert*-butyl alcohol at pH 7. The optical path length was 12.1 cm, λ = 430 nm, the dose was 1.7 μM, $I_0 = -893$ mV, and $\Delta I = 325$ mV. The inset shows a fit of the decomposition reaction to a first-order rate law.

of $[(OP)_2Cu^{2+}]$, [*tert*-butyl alcohol], wavelength, and pH over the range 4–10 (Table I). A typical kinetic plot is shown in Figure 2. The process observed cannot be attributed to the reaction of $(OP)_2Cu^+ + {}^{\bullet}CH_2C(CH_3)_2OH$, as its rate is independent of the pulse intensity, and it obeys a first-order rate law. In addition, the reaction is too slow, and the radicals would have disappeared much faster via reaction 8. It should be emphasized that the signal did not decay to zero, as can be seen in Figure 2. The spectrum of the final product was that of $(OP)_2Cu^+$, and OD_∞ depends on $[(OP)_2Cu^{2+}]$ and on the pulse intensity (Table I). When the ligand to metal ratio was 1:1, the signal was ca. 10% of that obtained when the ratio was 2.2 with the same kinetic behavior. Under this condition about 90% of the copper is in the form $(OP)Cu^{2+}$, the rest being $(OP)_2Cu^{2+}$.[14] Therefore, we assume that $(OP)Cu^+$ formed within the pulse is oxidized by $^{\bullet}CH_2C(CH_3)_2OH$ without any observable intermediate, and what we saw is the formation of the transient of $(OP)_2Cu^{2+}$ with a copper–carbon σ-bond.

When N_2O-saturated solutions containing 0.1–1 mM $(OP)_2Cu^{2+}$, 1–50 μM $(OP)_2Cu^+$, and 0.1–0.5 M *tert*-butyl alcohol at pH 7 are irradiated, the formation of an unstable intermediate is observed. The spectrum of this intermediate and the kinetics of its decomposition are identical with those obtained in the absence of $(OP)_2Cu^+$ in He-saturated solutions. A typical kinetic plot is given in Figure 3. The rate of the formation of the transient under all conditions was too fast to be measured. The small initial absorbance observed is due to the small difference in ε between $(OP)_2Cu^+$ and $(OP)_2Cu^{II}$–$CH_2C(CH_3)_2OH^+$ (Figure 1). The observation that the light transmittance at the end of the observed process is larger than that before the pulse indicates that $(OP)_2Cu^+$ is consumed in the observed process. The increase in light transmittance depends on $[(OP)_2Cu^{2+}]$, $[(OP)_2Cu^+]$, and the pulse intensity (Table II). The bleaching of the signal follows first-order kinetics with the same specific rate constant as in the former case, independent of $[(OP)_2Cu^{2+}]$, $[(OP)_2Cu^+]$, wavelength, and pulse intensity (Table II).

When N_2O-saturated solutions containing $(OP)_2Cu^{2+}$ and *tert*-butyl alcohol at pH 7 were pulse-irradiated, the behavior was

Table II. Values for the Observed Rate Constant of the Decomposition (k_d) of $(OP)_2Cu^{II}$–$CH_2C(CH_3)_2OH^+$ and the Percent Bleaching of $(OP)_2Cu^+$ in N_2O-Saturated Solutions Containing 0.1 M *tert*-Butyl Alcohol at pH 7 as a Function of Various Conditions[a]

$[Cu^{2+}]$, M	$[Cu^+]$, M	dose, M	λ, nm	OD_0	OD_∞	k_d, 10^3 s^{-1}	% yield
4.9×10^{-5}	1.3×10^{-6}	1.8×10^{-6}	430	0.006	−0.035	1.5	29
1.0×10^{-4}	2.2×10^{-6}	1.8×10^{-6}	430	0.005	−0.031	1.3	18
1.0×10^{-4}	2.2×10^{-6}	4.0×10^{-7}	430		−0.024	1.3	63
9.5×10^{-5}	2.8×10^{-6}	1.0×10^{-6}	430		−0.026	1.3	27
9.4×10^{-5} [b]	5.0×10^{-6}	3.3×10^{-6}	430		−0.061	1.6	20
9.4×10^{-5}	5.0×10^{-6}	1.0×10^{-6}	430		−0.036	1.4	38
9.4×10^{-5}	5.0×10^{-6}	3.0×10^{-7}	430		−0.017	1.2	60
9.1×10^{-5}	8.5×10^{-6}	1.4×10^{-6}	430	0.008	−0.055	1.7	41
8.9×10^{-5}	1.1×10^{-5}	1.6×10^{-6}	460		−0.047	1.9	39
8.3×10^{-5}	1.5×10^{-5}	6.0×10^{-7}	460		−0.027	1.5	57
1.0×10^{-3}	1.0×10^{-5}	1.3×10^{-6}	430	0.020	−0.005	2.5	<4
1.0×10^{-3}	4.8×10^{-5}	1.4×10^{-6}	530		−0.012	2.7	27

[a] The optical path length was 12.1 cm. [b] 0.5 M *tert*-butyl alcohol.

Table III. Values for the Observed Rate Constant of the Decomposition (k_d) of $(OP)_2Cu^{II}$–$CH_2CH_2OH^+$ in Ethylene-Saturated Solutions as a Function of Various Conditions[a]

$[(OP)_2Cu^{2+}]$, M	% ethylene	dose, 10^{-6} M	λ, nm	pH	OD_0	OD_∞	k_d, s^{-1}
5×10^{-5}	100	3.8	430	7	0.098	0.003	1.25×10^4
1×10^{-4}	100	3.8	430	7	0.122	0.004	1.02×10^4
1×10^{-4}	100	7.5	430	7	0.253	0.009	1.4×10^4
1×10^{-4}	100	7.5	340	7	0.117	0.01	1.13×10^4
1×10^{-4}	100	7.5	430	2.5	0.047	0.005	2.1×10^4
1×10^{-4}	100	3.8	430	4	0.115	0.004	1.28×10^4
1×10^{-4}	50[b]	3.8	430	7	0.124	0.006	8.2×10^3
1×10^{-4}	20[b]	7.5	430	7	0.263	0.012	7.8×10^3
1×10^{-4}	70[c]	3.8	430	7	0.021	0.002	1.24×10^4
2×10^{-4}	100	5.8	430	7	0.2	0.006	1.35×10^4
5×10^{-4}	100	3.8	430	7	0.129	0.008	1.03×10^4

[a] The optical path length was 12.1 cm. [b] Solutions saturated with ethylene were diluted with He-saturated solution. [c] 30% N_2O.

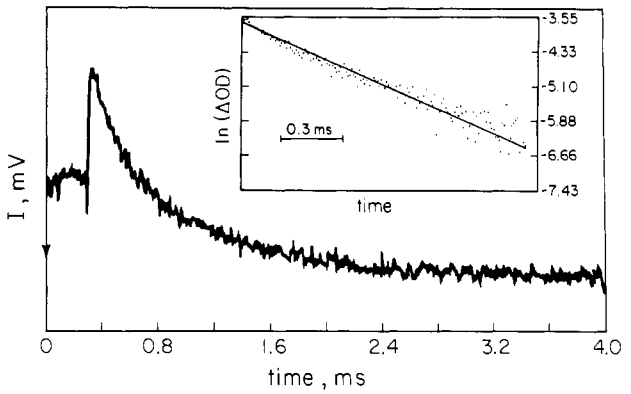

Figure 3. Typical kinetic plot of a pulse-radiolyzed N_2O-saturated solution containing 0.1 mM $(OP)_2Cu^{2+}$, 3 μM $(OP)_2Cu^+$, and 0.1 M *tert*-butyl alcohol butanol at pH 7. The optical path length was 12.1 cm, λ = 370 nm, the dose was 3 μM, $I_0 = -1114$, and $\Delta I = 41$ mV. The inset shows a fit of the increase in light transmittance to a first-order rate law.

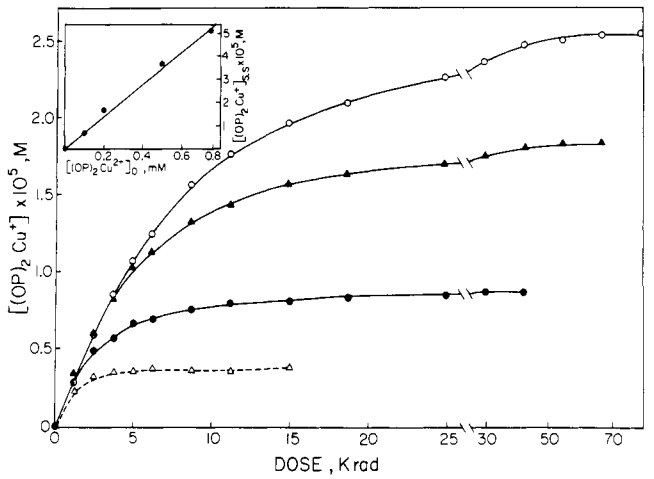

Figure 4. Dose dependence of $[(OP)_2Cu^+]$, formed in irradiated N_2O-saturated solutions containing various concentrations of $(OP)_2Cu^{2+}$ and 0.1 M *tert*-butyl alcohol at pH 7: △, 1×10^{-4} M $(OP)_2Cu^{2+}$; ●, 2×10^{-4} M $(OP)_2Cu^{2+}$; ▲, 5×10^{-4} M $(OP)_2Cu^{2+}$; ○, 7.5×10^{-4} M $(OP)_2Cu^{2+}$. The path length was 1 cm, λ = 430 nm, and the dose rate was 1.25 krads/min. The inset shows the dependence of $[(OP)_2Cu^+]_{ss}$ at saturation on the initial concentration of $(OP)_2Cu^{2+}$.

the same as in He-saturated solutions, but the signal was only ca. 8% of that observed in the He-saturated system. However, in these experiments the formation of $(OP)_2Cu^+$ was observed in the time scale of 1 s. The later process obeys first-order kinetics with a specific rate of 4.5 ± 1 s^{-1}, independent of $[(OP)_2Cu^{2+}]$ and $[(OP)_2Cu^+]$. The yield of $(OP)_2Cu^+$ was very low as compared to that of $^{\bullet}CH_2C(CH_3)_2OH$ produced during the pulse. Some steady-state experiments were carried out in N_2O-saturated solutions containing 0.1–0.75 mM $(OP)_2Cu^{2+}$ and 0.1 M *tert*-butyl alcohol at pH 7 by using γ-irradiation. It was found that $(OP)_2Cu^+$ is formed in these experiments and its concentration reaches a steady state. The steady-state concentration is linearly dependent on the initial concentration of $(OP)_2Cu^{2+}$ (Figure 4). From the slope of the lines at low doses $G((OP)_2Cu^+) = 2.2$ was determined, while in the case where *tert*-butyl alcohol is replaced by formate or methanol $G((OP)_2Cu^+) = 4.5$.[27]

(27) Johnson, G. R. A.; Nazhat, N. B. *J. Am. Chem. Soc.* **1987**, *109*, 1990.

The yield of 2-methylpropene was measured when solutions were pulsed and γ-irradiated. When N_2O-saturated solutions containing $(OP)_2Cu^{2+}$ and *tert*-butyl alcohol at pH 7 were irradiated, the yield of 2-methylpropene was dependent inversely on $[(OP)_2Cu^{2+}]$ and on the dose rate. The highest yield measured (ca. 20% of the radicals) was with γ-irradiation and 0.1 mM $(OP)_2Cu^{2+}$. Under the same conditions, but with He-saturated solutions, the yield was higher, ca. 60% of the radicals. When N_2O-saturated solutions containing also $(OP)_2Cu^+$ were γ-irradiated, the yield of 2-methylpropene was within experimental error equal to that of $^{\bullet}CH_2C(CH_3)_2OH$.

B. The Ethylene System. When ethylene-saturated solutions containing 5×10^{-5}–5×10^{-4} M $(OP)_2Cu^{2+}$ are irradiated, the formation of a short-lived transient was observed. The spectrum

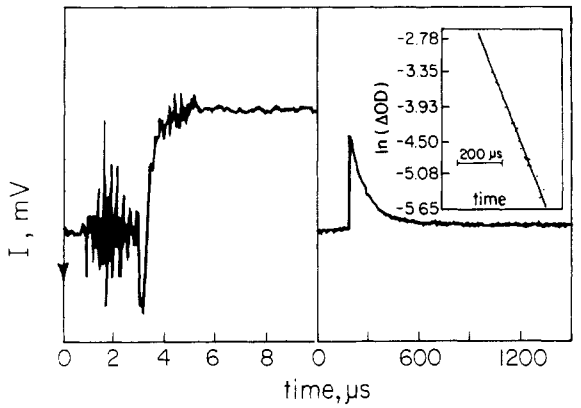

Figure 5. Typical kinetic plot of a pulse-radiolyzed ethylene-saturated solution containing 0.5 mM $(OP)_2Cu^{2+}$ at pH 7. The optical path length was 6.2 cm, the dose was 3.8 μM, λ = 430 nm, I_0 = 727 mV, and ΔI = 116 and 102 mV for the formation and the decomposition traces, respectively. The inset shows a fit of the decomposition reaction to a first-order rate law.

of the transient, which is attributed to $(OP)_2Cu^{II}$–$CH_2CH_2OH^+$, is given in Figure 1. The formation of the intermediate was too fast to be followed. A typical kinetic plot is given in Figure 5. The kinetics of the decomposition of the transient with the copper–carbon σ-bond obeys a first-order rate law, independent of $[(OP)_2Cu^{2+}]$, wavelength, and pH (4 – 7) and slightly dependent on $[CH_2{=}CH_2]$ and on the pulse intensity (Table III). When the same solutions were saturated with a mixture of $CH_2{=}CH_2/N_2O$ with a ratio of 7:3, the same signal was observed, but it was ca. 8% of that obtained in ethylene-saturated solutions (Table III). In this case e_{aq}^- and OH• are converted into $•CH_2CH_2OH$ radicals and H• is converted into $•CH_2CH_3$ radicals.

The yield of ethylene as a final product was measured in irradiated He-saturated solutions containing $(OP)_2Cu^{2+}$ and 0.1 M ethanol at pH 7. Under these conditions 13.2% of OH• yields the β-radical, $•CH_2CH_2OH$, and the rest the α-radical, CH_3CHOH.[23,28] The yield of ethylene was within experimental error equal to that predicted for the β-radicals.

Discussion

The kinetic results indicate that, within the pulse, short-lived intermediates are formed from $(OP)_2Cu^+$ and $•CH_2C(CH_3)_2OH$ or $•CH_2CH_2OH$ radicals. The observation that the first absorption band of these intermediates is similar to that of $(OP)_2Cu^+$ indicates that the binding of the alkyl to the copper ions has only a minor effect on the energy of the highest occupied orbital of the copper ions. The transients formed decompose via first-order reactions with rates being independent of [R•], $[(OP)_2Cu^{2+}]$, $[(OP)_2Cu^+]$, wavelength, and pH (4–10) and slightly dependent on the pulse intensity. The product analysis shows that 2-methylpropene and ethylene are formed. The yield of 2-methylpropene depends inversely on the dose rate and on $[(OP)_2Cu^{2+}]$, and at low concentrations on $[(OP)_2Cu^+]$. When the dose rate is very low (γ-irradiation) and the solutions contain $(OP)_2Cu^+$, the yield of 2-methylpropene was equal to the yield of $•CH_2C(CH_3)_2OH$, as in the absence of OP.[13] According to these results, $(OP)_2Cu^{II}$–$CH_2C(CH_3)_2OH^+$ undergoes a β-hydroxyl elimination reaction via the mechanism

$$(OP)_2Cu^{II}{-}CH_2C(CH_3)_2OH^+ \rightleftharpoons (OP)_2Cu^+ + •CH_2C(CH_3)_2OH \quad (-12)$$

$$(OP)_2Cu^{II}{-}CH_2C(CH_3)_2OH^+ \rightarrow (OP)_2Cu^{2+} + CH_2{=}C(CH_3)_2 + OH^- \quad (13)$$

$$(OP)_2Cu^{2+} + •CH_2C(CH_3)_2OH \rightarrow (OP)_2Cu^+ + \text{products} \quad (14)$$

We were unable to follow the mechanism of the reduction of $(OP)_2Cu^{2+}$ by $•CH_2C(CH_3)_2OH$ using the pulse radiolysis technique because the reaction occurs without any observable intermediate and also because the absorbance of $(OP)_2Cu^{II}$-$CH_2C(CH_3)_2OH^+$ is high in the spectral region studied. The results with γ-radiolysis point toward the fact that part of the $(OP)_2Cu^{2+}$ is reduced by $•CH_2C(CH_3)_2OH$ to $(OP)_2Cu^+$. Even under conditions of γ-radiolysis, where reaction 8 can be neglected, the yield of $(OP)_2Cu^+$ is ca. 60% of that obtained when *tert*-butyl alcohol is replaced by formate or methanol, taking into account that H_2O_2 generated during the irradiation lowers the yield of $(OP)_2Cu^+$.[27]

Assuming a steady-state approximation for $[•CH_2C(CH_3)_2OH]$, the rate equation (15) is obtained for the decomposition of

$$-d[Cu^{II}{-}R]/dt = \{(k_{12}k_{13}[Cu^+] + k_{14}(k_{13} + k_{-12})[Cu^{2+}])/(k_{12}[Cu^+] + k_{14}[Cu^{2+}])\}[Cu^{II}{-}R] \quad (15)$$

$(OP)_2Cu^{II}$–$CH_2C(CH_3)_2OH^+$. Under γ-radiolysis we assume a steady-state approximation for $[(OP)_2Cu^{II}{-}R]$. At high doses $[(OP)_2Cu^+]$ reaches saturation (Figure 4), and eq 16 is obtained,

$$[(OP)_2Cu^{2+}]_0/[(OP)_2Cu^+]_{ss} = k_{12}k_{13}/(k_{-12} + k_{13})k_{14} - 1 \quad (16)$$

where $[(OP)_2Cu^{2+}]_0$ is the initial concentration of $(OP)_2Cu^{2+}$. From the slope of the line in the inset of Figure 4 we obtain

$$k_{12}k_{13}/(k_{-12} + k_{13})k_{14} = 30 \quad (17)$$

The formation of the transient with a copper–carbon σ-bond is very fast, and k_{12} is estimated to be larger than 10^{10} M^{-1} s^{-1}. Assuming that $k_{-12} < k_{13}$, the rate equation (15) reduces approximately to the rate equation (18), and from eq 17 we obtain

$$-d[Cu^{II}{-}R]/dt = k_{13}[Cu^{II}{-}R] \quad (18)$$

$k_{12}/k_{14} = 30$, and hence $k_{14} > 3 \times 10^8$ M^{-1} s^{-1}. If, on the other hand, we assume that $k_{-12} > k_{13}$, then from eq 17 we obtain $k_{14} = k_{12}k_{13}/30k_{-12}$. As a result, $k_{14} < 3 \times 10^8$ M^{-1} s^{-1}, and under our experimental conditions, $k_{12}[(OP)_2Cu^+] > k_{14}[(OP)_2Cu^{2+}]$. In this case we will get the rate equation (18) only if we also assume that $k_{13} > k_{14}k_{-12}[(OP)_2Cu^{2+}]/k_{12}[(OP)_2Cu^+]$ and, by rearranging, that $k_{12}[(OP)_2Cu^+] > (k_{14}k_{-12}/k_{13})[(OP)_2Cu^{2+}]$, which cannot be correct, since $k_{12}[(OP)_2Cu^+] > k_{14}[(OP)_2Cu^{2+}]$, and we assumed that $k_{-12} > k_{13}$. As the results show that the rate of the decomposition reaction is independent of $[(OP)_2Cu^{2+}]$ and $[(OP)_2Cu^+]$, we must conclude that the assumption that $k_{-12} < k_{13}$ seems to be correct, and therefore, $k_{13} = (1.7 \pm 0.4) \times 10^3$ s^{-1}, $k_{14} > 3 \times 10^8$ M^{-1} s^{-1}, $k_{12} > 10^{10}$ M^{-1} s^{-1}, and hence $K_{12} > 6 \times 10^6$ M^{-1}.

In the case of $(OP)_2Cu^{II}$–$CH_2CH_2OH^+$, no effect of $[(OP)_2Cu^{2+}]$ and pulse intensity on the final yield of $(OP)_2Cu^+$ is observed. In fact, no $(OP)_2Cu^+$ is observed as a final product. Thus, the mechanism of the decomposition would be via reaction 13a, and hence, we must assume that $k_{-12a} \ll k_{13a}$, and therefore

$$(OP)_2Cu^{II}{-}CH_2CH_2OH^+ \rightleftharpoons (OP)_2Cu^+ + •CH_2CH_2OH \quad (-12a)$$

$$(OP)_2Cu^{II}{-}CH_2CH_2OH^+ \rightarrow (OP)_2Cu^{2+} + CH_2{=}CH_2 + OH^- \quad (13a)$$

$k_{13a} = (1.1 \pm 0.3) \times 10^4$ M^{-1} s^{-1}; i.e., the stability constant for the binding of $•CH_2CH_2OH$ to $(OP)_2Cu^+$ is considerably larger than that of $•CH_2C(CH_3)_2OH$.

The rate of the β-hydroxyl elimination reaction in the case of $(OP)_2Cu^{II}$–$CH_2C(CH_3)_2OH^+$ is pH-independent between pH 4 and pH 10, indicating that the acid-dependent term cannot exceed 5×10^6 M^{-1} s^{-1}. In the case of $(OP)_2Cu^{II}$–$CH_2CH_2OH^+$, it cannot exceed 2×10^6 M^{-1} s^{-1}, while in the absence of OP, it is 8.6×10^7[13] and 3.8×10^7 M^{-1} s^{-1}[7] for *tert*-butyl alcohol and ethylene systems, respectively. The corresponding pH-independent terms are 1.7×10^3 and 1.1×10^4 s^{-1}, while in the absence of OP values of 5×10^4[13] and 3.2×10^3 s^{-1}[7] were obtained for the *tert*-butyl alcohol and ethylene systems, respectively. Thus, coordination of OP to copper affects the specific rate constants of both the acid-independent and acid-dependent reactions. The source of this effect is under study.

(28) Asmus, K. D.; Meckel, H.; Henglein, H. *J. Phys. Chem.* **1973**, *77*, 1218.

The results show that $(OP)_2Cu^+$ reacts with β-hydroxyl radicals to form intermediates with copper–carbon σ-bonds, which decompose via β-hydroxyl elimination reactions. It will be very interesting to find out whether $(OP)_2Cu^+$ reacts also with free radicals formed in biological systems to produce transients with copper–carbon σ-bonds. If this is the case, one of the routes for biological damage may occur through such intermediates.

Acknowledgment. This study was supported by The Council of Tobacco Research, The Israel Academy of Science, The Israel USA BNF, The Israel Atomic Energy Commission, and the Planning and Granting Committee of the Council of Higher Education. We wish to thank D. Carmi, Y. Nehemia, and Y. Nahon for technical assistance. D.M. wishes to thank I. Evans for her interest and support.

Contribution from the Department of Chemistry and Biochemistry, University of Maryland, College Park, Maryland 20742

Preparation and Configurational Analysis of the Stereoisomers of β,γ-Bidentate $Rh(H_2O)_4ATP$ and α,β,γ-Tridentate $Rh(H_2O)_3ATP$. A New Class of Enzyme Active Site Probes[‡,1]

Zichun Lu, Andrew L. Shorter,[†] Irene Lin,[†] and Debra Dunaway-Mariano*

Received June 3, 1988

Reaction of $[Rh(H_2O)_6](ClO_4)_3$ with adenosine 5′-triphosphate (ATP) at pH 3 and 80 °C generated a mixture of β,γ-bidentate $Rh(H_2O)_4ATP$ and α,β,γ-tridentate $Rh(H_2O)_3ATP$ in a 1:1 ratio. Purification of the two structural forms was accomplished on a Sephadex-G10 gel filtration column (yield of each purified isomer ≈ 10%). The two β-P epimers (Δ and Λ) of the β,γ-bidentate $Rh(H_2O)_4ATP$ complex were resolved on a reverse-phase HPLC column as were the four α,β,γ-tridentate $Rh(H_2O)_3ATP$ diastereoisomers (β-P Δ, α-P endo; β-P Δ, α-P exo; β-P Λ, α-P endo; β-P Λ, α-P exo). β,γ-Bidentate $Rh(H_2O)_4ATP$ isomer **1** (the first of the two isomers to elute from the HPLC column) was found to be a substrate for pyruvate kinase but not to be a substrate for hexokinase. Isomer **2**, on the other hand, served as a substrate for hexokinase, but it was not a substrate for pyruvate kinase. On the basis of the known stereochemical specificities of these two enzymes, isomer **1** was assigned the Δ configuration and isomer **2**, the Λ configuration. The Δ-bidentate isomer displayed a (−) Cotton effect at the 425-nm λ_{max} ($\theta = -380$ deg cm^2 dmol^{-1}), while the Λ isomer displayed a (+) Cotton effect ($\theta = +180$ deg cm^2 dmol^{-1}) at this wavelength. The configuration of the β-P in the four α,β,γ-tridentate $Rh(H_2O)_3ATP$ isomers was determined by separately converting the Δ and Λ bidentate isomers to the corresponding pairs of tridentate α-P epimers. The Δ isomer gave rise to tridentate isomers **1** and **4**, and the Λ isomer gave rise to tridentate isomers **2** and **3**. So to determine the α-P configuration in the four tridentate isomers, α,β,γ-tridentate $Rh(H_2O)_3((R_p)$-[α-^{16}O,^{18}O]ATP) was prepared and the magnitudes of the ^{18}O-induced chemical shifts of the α-P resonances observed in the ^{31}P NMR spectrum of the mixture of stereoisomers were measured. On the basis of these measurements the isomer configurations were shown to be as follows: isomer **1**, β-P Δ, α-P exo; isomer **2**, β-P Λ, α-P exo; isomer **3**, β-P Λ, α-P endo; isomer **4**, β-P Δ, α-P endo. Both tridentate isomers having the Δ β-P configuration showed negative Cotton effects at the 450-nm λ_{max} (for **1** −340 and for **4** −500 deg cm^2 dmol^{-1}) and positive Cotton effects at the 400-nm λ_{max} (for **1** +1400 and for **4** +980 deg cm^2 dmol^{-1}), while the tridentate isomers having the Λ-β configuration displayed positive Cotton effects at the 450-nm λ_{max} (for **2** +250 and for **3** +450 deg cm^2 dmol^{-1}) and negative Cotton effects at the 400-nm λ_{max} (for **2** −960 and for **3** −480 deg cm^2 dmol^{-1}). The bidentate and tridentate $Rh(H_2O)_nATP$ isomers were found to be most stable at low pH and low temperature. At 80 °C the conversion of the bidentate form to the tridentate form occurred significantly faster than did epimerization at the β-P of either structural isomer ($t_{1/2}$ of bidentate $Rh(H_2O)_4ATP$ at pH 3 is ~5 min). At higher pH (e.g. pH 6–7) solutions of bidentate or tridentate $Rh(H_2O)_nATP$ were found to equilibrate comparatively faster (at pH 6 and 25 °C $t_{1/2}$ of bidentate $Rh(H_2O)_4ATP$ is ~1 h and $K_{eq} \approx 1$). However, at low temperature the isomerization rate was found to be slow enough to allow the utilization of the individual isomers of the $Rh(H_2O)_nATP$ complexes as structural and biochemical probes of MgATP.

Introduction

Exchange-inert Co(III) and Cr(III) complexes of polyphosphates (e.g. ATP and ADP) have proven to be useful probes of the structural and biochemical properties of naturally occurring Mg^{II}(polyphosphate) complexes.[2] Because these complexes are stable in aqueous solution, they can be used to determine the structure and stereochemistry of the kinetically labile Mg^{II}(polyphosphate) complex that serves as the natural substrate for a given enzyme. The exchange-inert complexes have also been successfully used in the study of the kinetic mechanisms, metal ion cofactor requirements, and the substrate and cofactor binding sites of Mg^{II}(polyphosphate) processing enzymes.[2]

However, the application of the Cr(III) and Co(III) complexes as structural and biochemical probes does have some serious limitations. For example, NMR methods cannot be used to characterize Cr^{III}(polyphosphate) probes or their enzymic products owing to the paramagnetic nature of the Cr(III) metal. The Co^{III}(polyphosphate) complexes on the other hand are diamagnetic and are therefore easily characterized by NMR techniques, but the redox properties of the metal require that the Co^{III}(polyphosphate) complexes also be coordinated to nitrogen-containing ligands such as NH_3. In many cases the NH_3 ligands interfere with tight and productive binding of the $Co^{III}(NH_3)_n$(polyphosphate) complex to the enzyme and for this reason use of these systems as biochemical probes is restricted.

* To whom correspondence should be addressed.
† Current address: I.L., Development Center for Biotechnology, 81 Chang Hing St., Taipei, Taiwan; A.L.S., Smith Klein and French Co., Philadelphia, PA 19101.

‡ This work was supported in part by National Institutes of Health Grant GM-28688 and American Heart Association Grant 86992. D.D.-M. acknowledges a Research Career Development Award from the National Institutes of Health (ES-00111) and a Fellowship Award from the Alfred P. Sloan Foundation. A.L.S. acknowledges support by a Postdoctoral Fellowship from the Maryland Chapter of the American Heart Association. The National Science Foundation is acknowledged for support for purchase of the Bruker 400-MHz nuclear magnetic resonance spectrometer (Grant DMB-84-20175) used in these studies.

(1) Abbreviations: adenosine 5′-triphosphate, ATP; adenosine 5′-diphosphate, ADP; adenosine 5′-phosphate, AMP; potassium 2-morpholinoethanesulfonate, K(MES); mixture of β,γ-bidentate $Rh(H_2O)_4ATP$ and α,β,γ-tridentate $Rh(H_2O)_3ATP$, $Rh(H_2O)_nATP$; nuclear magnetic resonance, NMR; high-pressure liquid chromatography, HPLC; circular dichroism, CD.

(2) For recent reviews see: Cleland, W. W. *Methods Enzymol.* **1982**, *87*, 159. Cleland, W. W. In *Mechanisms of Enzymatic Reactions: Stereochemistry*; Frey, P. A., Ed.; Elsevier: New York, 1985; pp 141–148. Dunaway-Mariano, D. *Ibid.* pp 149–164.

0020-1669/88/1327-4135$01.50/0